ARTICLE

Green Mechanochemical Synthesis of Imine-Linked Covalent Organic Frameworks for High Iodine Capture

Received 00th January 20xx,
Accepted 00th January 20xx

DOI: 10.1039/x0xx00000x

Normanda Brown,[a] Ziad Alsudairy,[a] Ranjan Behera,[b] Fazli Akram,[a] Kuangcai Chen,[c] Kayla Smith-Petty,[a] Bria Motley,[a] Spirit Williams,[a] Wenyu Huang,[b] Conrad Ingram,[a] Xinle Li*[a]

Covalent organic frameworks (COFs) have emerged as promising adsorbents for radioiodine capture. However, the conventional solvothermal synthesis contradicts the principles of green chemistry due to the use of hazardous solvents, long reaction times (typically 3 days), and high reaction temperatures. To address these issues, we demonstrate for the first time the green, efficient, liquid-assisted mechanochemical synthesis of COF adsorbents for high iodine capture. The ball milling mechanochemical synthesis was performed with various liquid additives at ambient temperature, yielding six imine-linked COFs of diverse pore sizes and functionalities in merely 1 hour. Notably, one representative COF exhibited high crystallinity and a remarkable surface area of 1387 $m^2 g^{-1}$ in just 1 minute of ball milling. When tested as adsorbents for static iodine vapor capture at 75 °C, four mechanochemically synthesized COFs exhibited outstanding iodine adsorption capacities of 6.4-7.1 g g^{-1}, comparable to or exceeding those of solvothermally synthesized COF and most reported COF adsorbents. Furthermore, Fourier transform infrared and X-ray photoelectron spectroscopy corroborated the charge transfer between iodine and COF adsorbents. This mechanochemical methodology will pave the path for green, rapid, facile, and scalable synthesis of COFs, revealing great prospects for applications in environmental remediation and beyond.

Introduction

Nuclear energy is deemed a safer and cleaner source of energy than fossil fuels, solar, and wind, contributing to approximately 11% of the world's electricity. As such, it offers a viable and sustainable path towards achieving carbon neutrality goals by the mid-century.[1] However, the radionuclides generated from nuclear power operations pose a substantial threat to human health and the ecosystem. Previous generations have suffered the consequences of nuclear accidents such as the Mayak facility in Russia (1948)[2], and the Chornobyl disaster (1986).[3] More recently, the Fukushima Daiichi nuclear disaster (2011) discharged over 10^{19} Bq of radionuclides into the environment, leading to severe contamination in surrounding areas.[4] To safeguard the ecosystem, it is imperative to take immediate action to sequester radionuclides effectively. Among the various radionuclides, radioiodine is especially hazardous due to its high activity, volatile nature, long-term risk, and adverse health effects. The two main forms of radioiodine isotopes, ^{129}I and ^{131}I, are fission byproducts of the nuclear energy cycle, with half-lives of 15.7 million years and 8.02 days, respectively. Excessive exposure to them can engender severe diseases such as hyperthyroidism and thyroid cancer.

Accordingly, the effective removal of radioiodine has drawn worldwide attention in recent years. Among many techniques for removing radioiodine, adsorptive removal is of particular interest due to its low cost, ease of operation, and high energy efficiency. Unfortunately, traditional adsorbents such as activated carbon, silver-doped zeolites, and mesoporous silica are impractical due to their low adsorption capacity and high regeneration cost.[5] New porous adsorbents such as metal-organic frameworks (MOFs) possess low adsorption capacities and limited chemical stability caused by the metal secondary building units. Alternatively, porous organic polymers (POPs) composed solely of light elements (C, H, N, O, S, B, etc.) have emerged as auspicious adsorbents.[6] Unlike amorphous polymers, covalent organic frameworks (COFs) are a burgeoning class of crystalline POPs with precise integration of organic units into high-order networks.[7] Compared to other benchmark porous materials such as zeolites, amorphous POPs, and MOFs, COFs have unparalleled structural advantages including ultralow density, regular networks, high porosity, exceptional structural modularity, and superb synthetic versatility, which underpin their broad applications in gas storage, catalysis, energy storage, water harvesting, environmental remediation, etc.[8-11] Since the first report of using COFs as iodine adsorbents in 2017,[12] enormous scientific efforts have been devoted to the fabrication of high-performance COF adsorbents through three main routes: (1) *de novo* synthesis of COF adsorbents containing iodine affinity sites such as imine,[13-15] hydrazone,[16] cationic species,[17] amino,[18] hydrazides,[19] thiophene,[20] tetrathiafulvalene,[21] phosphine;[22] (2) grafting ionic groups onto already-synthesized COFs by post-synthetic modification;[23] and (3) constructing hierarchically porous COFs

[a] *Department of Chemistry, Clark Atlanta University, Atlanta, Georgia 30314, United States*
[b] *Department of Chemistry, Iowa State University, Ames, Iowa 50011, United States.*
[c] *Department of Chemistry and Imaging Core Facility, Georgia State University, Atlanta, Georgia 30303, United States.*
*Corresponding author. Email: xli1@cau.edu

through supercritical CO_2 drying,[24] freeze-drying,[25] and template-assisted modulated synthesis.[26] Despite substantial advances, the synthesis of COF adsorbents still heavily relies on conventional solvothermal synthesis, which entails multiday synthesis, the usage of toxic organic solvents, high temperatures, and anaerobic conditions.[27] These issues contradict the core principles of green chemistry and pose considerable obstacles to the further applications of COFs. Hence, it is imperative to pursue a green methodology for synthesizing COFs, one that uses minimal hazardous solvents, operates at mild reaction temperatures and reduces reaction times while retaining high efficacy.

In the quest for sustainable and eco-friendly synthetic methods,[28-29] mechanochemical synthesis has gained enormous attention.[30] This approach harnesses mechanical forces such as compression and shear to induce chemical transformation and has been recognized by the IUPAC as one of ten world-changing technologies.[31] Mechanochemical synthesis offers numerous advantages, including shortened reaction times, mild conditions, augmented efficiency, solventless condition, simple operation, sustainability, and high scalability.[32] This synthetic methodology upholds the principles of green chemistry and has advanced rapidly in the realm of chemistry and materials science. Through green mechanochemical synthesis, a myriad of chemical products such as fine chemicals, pharmaceuticals, nanoparticles, and polymers have been successfully synthesized. Among the wide array of products, porous materials such as porous carbons, zeolites, POPs, polymers of intrinsic microporosity (PIMs), and MOFs have garnered considerable attention.[33-35] In 2013, Banerjee's group embarked on the first neat mechanochemical synthesis of *β*-ketoenamine-linked COFs by manually grinding monomers with a mortar and pestle.[36] To further optimize mechanochemical conditions, they first employed a liquid-assisted grinding (LAG) strategy to synthesize COFs bearing *β*-Ketoenamine, imine, and hydrazone linkages in 2014.[37] Later in 2017, they developed a rapid mechanochemical synthesis of twelve *β*-ketoenamine-linked COFs using *p*-toluene sulfonic acid as a molecular organizer.[38] Recently in 2021, Lotsch's group provided the first real-time mechanistic insight into the mechanochemical imine COF formation via *in situ* X-ray diffraction and Raman spectroscopy.[39] Although mechanochemistry holds great promise as a green alternative to conventional solvothermal routes, its broad utility in COF synthesis is still in its infancy. Moreover, mechanochemically synthesized COFs are mainly utilized in specific areas such as proton-conducting solid electrolytes,[40] electrodes,[41] water sorption,[38] solid phase extraction,[42] and catalysis.[43] Thus, expanding their use to address pressing social needs will certainly unleash the vast potential of mechanochemical synthesis.

In this study, we present the first green mechanochemical synthesis of COF adsorbents (designated as MC-COFs, Scheme 1) for highly efficient iodine capture. The optimized synthetic route for the imine-linked COFs was systematically investigated based on the liquid additive, catalyst selection, number and size of milling balls, milling frequency, and reaction time. Under optimized mechanochemical conditions, a library of six 2D hexagonal imine-linked COFs was synthesized within an hour, exhibiting high crystallinity, permanent porosity, varied pore sizes, and diverse functionalities. Notably, one representative COF (MC-DMTP-TPB COF) displayed high crystallinity and surface area as high as 1387 m^2 g^{-1} in just 1 minute of ball milling. Additionally, four MC-COFs demonstrated outstanding iodine adsorption capacities of 6.6-7.1 g g^{-1} at 75 °C, equivalent to or surpassing those of traditionally synthesized COF and most reported COF adsorbents. Moreover, MC-DMTP-TPB COF retained high iodine uptake (> 5.8 g g^{-1}) after three successive adsorption-desorption cycles. Lastly, the underlying mechanism of iodine adsorption was investigated through X-ray photoelectron spectroscopy and Fourier transform infrared (FTIR) analyses.

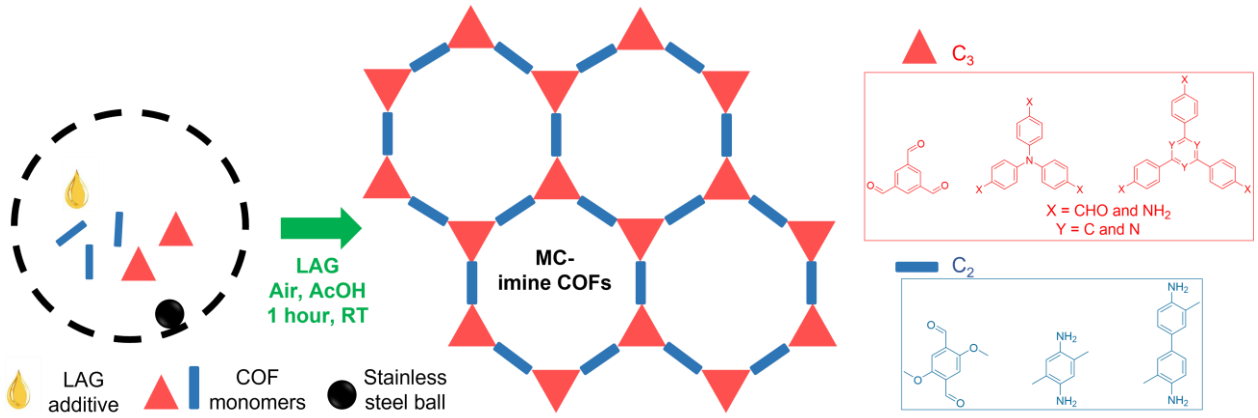

Scheme 1. Schematics of the green, rapid, general, and ambient-temperature synthesis of imine-linked 2D hexagonal COFs using liquid-assisted grinding (LAG) mechanochemistry.

Results and discussion

To test the feasibility of our mechanochemical approach, we selected a prototypical imine-linked 2D COF, DMTP-TPB COF, which is composed of 2,5-dimethoxybenzene-1,4-carboxaldehyde (DMTP) and 1,3,5-tris(4-aminophenyl) benzene (TPB).[44] The initial study

showed that this COF, termed MC-DMTP-TPB COF (Fig. 1a), was readily obtained via a ball milling method. Thus, this COF was used as a model system to optimize the mechanochemical parameters. All mechanochemical syntheses were carried out in a 5-mL stainless steel milling jar in a Retsch MM400 Mixer Mill machine (Fig. 1a, inset) unless otherwise specified.

Given that the liquid-assisted grinding (LAG) strategy has been demonstrated to be advantageous for the construction of porous materials compared to neat mechanochemical synthesis,[37, 40, 45] we initially investigated the effect of liquid additives on the formation of COFs. Powder X-ray diffraction (PXRD) analysis revealed that the LAG exerted a profound effect on the crystallinity of MC-DMTP-TPB COF, as milling without a liquid additive did not generate any crystalline product (Fig. S1). To meet the requirements of LAG, the ratio (η) of liquid additive (μL) to reactant (mg) was kept below 1 μL/mg. Several common organic solvents including dioxane, dichlorobenzene/*n*-butanol, *n*-butanol, acetonitrile, and benzonitrile were tested (Fig. 1b). Among these solvents, acetonitrile was found to be the optimal LAG additive. Moreover, the amount of LAG additive was crucial to the crystallinity of COFs. Increasing the amount of acetonitrile (η < 1 μL/mg) resulted in COFs with higher crystallinity (Fig. S1).

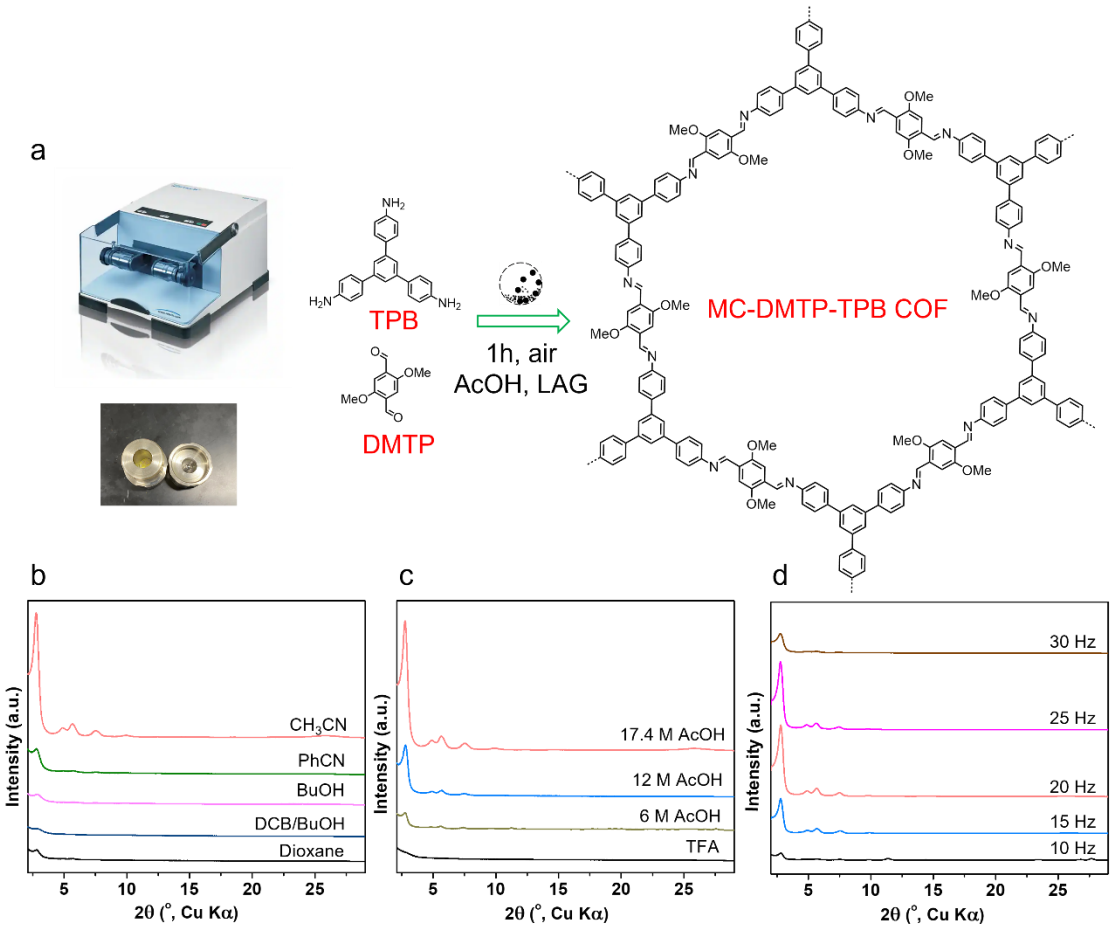

Fig. 1. Effect of synthesis variables on the crystallinity of MC-DMTP-TPB COF made by LAG mechanochemistry. (a) Liquid-assisted mechanochemical synthesis of MC-DMTP-TPB COF. Inset is the Retsch MM400 Mixer Mill and 5-mL stainless steel milling jar. (b) PXRD patterns of MC-DMTP-TPB COF using different LAG additives, (c) different catalysts, and (d) milling frequency.

The effect of acetic acid (AcOH) concentration (6 M, 12 M, and 17.4 M) on the formation of MC-DMTP-TPB COF was investigated. PXRD analysis showed that the glacial AcOH (17.4 M) generated the most crystalline COF compared to 6 M and 12 M AcOH (Fig. 1c). It was also observed that the reaction did not proceed in the absence of AcOH, highlighting the indispensable role of the catalyst in the mechanochemical synthesis of COFs. In addition, the use of trifluoroacetic acid (TFA) failed to produce crystalline COF. Interestingly, the size and number of grinding balls also had a considerable effect on the crystallinity of COFs. Ball milling with a small ball (5 mm in diameter) led to superior crystallinity of COF compared to larger ones (7 and 10 mm) under the same conditions (Fig. S2). Furthermore, using only 1 grinding ball resulted in higher crystallinity compared to 2 and 3 balls under ball milling (Fig. S3). Among various milling frequencies tested (10, 15, 20, 25, and 30 Hz), 20 Hz was found to be the optimal frequency for the formation of MC-DMTP-TPB COF, revealing the highest crystallinity (Fig. 1d). To assess the potential scalability of the mechanochemical methodology, the reaction was scaled up 25-fold in a large milling jar (25 mL), leading to approximately ~0.9 g of MC-DMTP-TPB COF with a good yield (83%), broadened peak widths, and high crystallinity compared to the small-scale reaction (Fig. S4).

Under the optimized condition, MC-DMTP-TPB COF was obtained by milling DMTP (0.105 mmol) with TPB (0.07 mmol) in the presence of glacial acetic acid (15 µL) as a catalyst and acetonitrile (30 µL) as a LAG additive (η = 1 µL/mg). The reaction mixture was milled at 20 Hz for 1 hour in a 5-mL stainless steel milling jar with a 5 mm steel ball, affording yellowish solids in quantitative yields. The progression of the Schiff-base reaction was assessed by FTIR spectroscopy. In the FTIR spectra, MC-DMTP-TPB COF displayed the emergence of C=N stretch (1615 cm^{-1}) and the disappearance of N–H stretch (3100-3300 cm^{-1}) in the starting monomer TPB (Fig. S5), indicating the successful occurrence of Schiff-base reaction under the developed mechanochemical condition. The crystallinity of MC-DMTP-TPB COF was verified by PXRD analysis, which revealed an intense diffraction peak at 2.8° along with minor peaks at 4.9, 5.7, 7.5, 9.9, and 25.9°, corresponding to the (100), (110), (200), (210), (220), and (001) reflection planes, respectively (Fig. 1b). The experimental PXRD pattern coincided well with that reported in the literature. Thermogravimetric analysis (TGA) indicated that MC-DMTP-TPB COF was thermally stable up to 400 °C under N_2 (Fig. S6). In addition, MC-DMTP-TPB COF exhibited exceptional chemical stability and retained crystallinity after exposure to 12 M HCl and 14 M NaOH aqueous solutions for 7 days (Fig. S7), which is consistent with the solvothermally synthesized DMTP-TPB COF in previous report.[44]

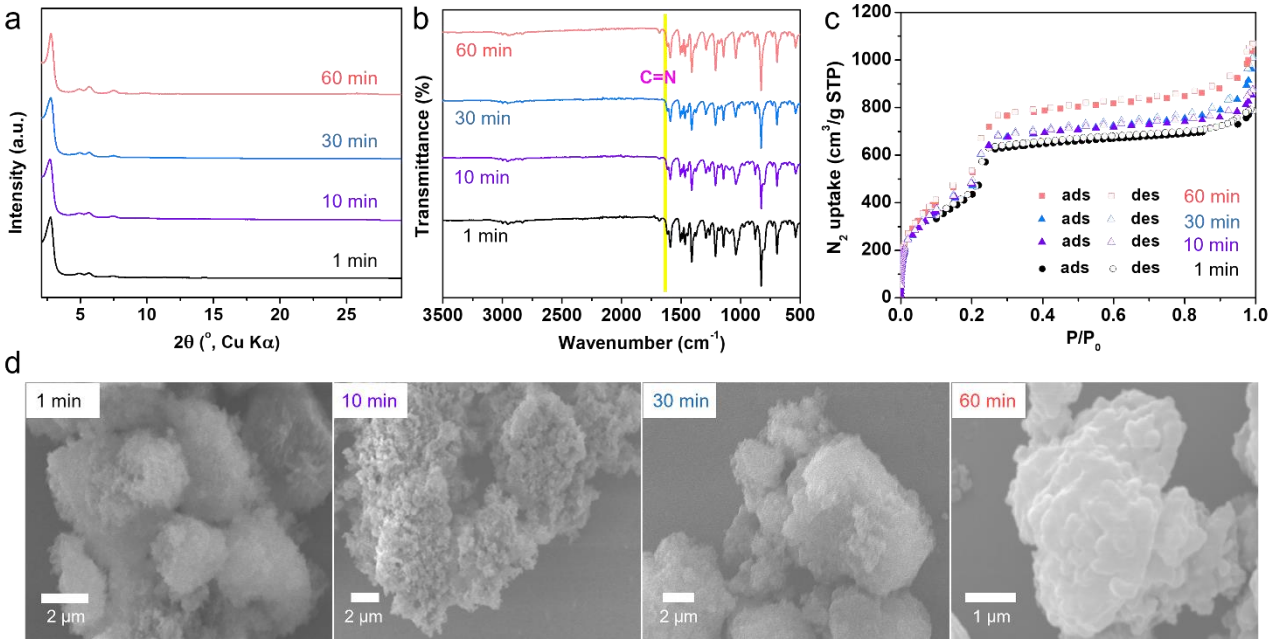

Fig. 2. Progression of MC-DMTP-TPB COF made by LAG mechanochemistry. (a) PXRD patterns. (b) FTIR spectra, (c) N_2 adsorption-desorption isotherms, and (d) SEM images of MC-DMTP-TPB COF at different milling times.

To gain insight into the mechanochemical synthesis, we monitored the progression of MC-DMTP-TPB COF at various milling times using *ex situ* PXRD, FTIR, N_2 adsorption, and SEM analyses (Fig. 2). Intriguingly, PXRD and FTIR analyses verified the formation of highly crystalline COF after just 1 minute of milling with a moderate yield of 56% (Figs. 2a-2b), which underlines the high efficiency of the mechanochemical synthesis. As the milling time increased, both the yields (89% for 10 minutes, 95% for 30 minutes, and 98% for 60 minutes) and crystallinity improved gradually (Fig. 2a). The permanent porosity and surface area of MC-DMTP-TPB COFs at different milling times were examined by N_2 adsorption analysis at 77 K. All COFs displayed a reversible type-IV adsorption isotherm (Fig. 2c), indicative of the mesoporous character. Strikingly, MC-DMTP-TPB COF formed within 1 minute displayed a high Brunauer-Emmett-Teller (BET) surface area of 1387 $m^2 g^{-1}$. As the milling time increased to 10, 30, and 60 minutes, the surface areas progressively increased to 1400, 1517, and 1554 $m^2 g^{-1}$, respectively. Moreover, the pore size distribution of MC-DMTP-TPB COFs prepared at different milling times (Figure S8) was estimated by fitting the isotherms using quenched solid density functional theory (QSDFT). The analysis exhibited similar pore width centered around 3.2 nm, which is consistent with the previously reported value.[44] Although BET surface areas are smaller compared to those solvothermally synthesized DMTP-TPB COFs (1760 and 2105 $m^2 g^{-1}$),[44, 46] the rapid synthesis time (< 60 minutes), ambient condition, quantitative yields, and nearly solventless nature make the mechanochemical approach highly appealing. It is worth noting that MC-DMTP-TPB COF represents a rare COF that attains high crystallinity and porosity in an exceptionally short time (1 minute) and at ambient temperature. A summary of rapidly synthesized COFs at ambient temperature can be found in Table S1. Notably, our approach differs from the previous mechanochemical synthesis of *β*-ketoenamine-linked COFs, which necessitated additional heating treatment at 170 °C after 1 minute-grinding.[38] We also investigated the morphological evolution of COF particles during the reaction (Fig. 2d). SEM images revealed agglomerated crystallites with varying shapes in MC-DMTP-TPB COFs. As the milling time increased, the length of these crystallites increased from sub-micron size to ~1 µm (Fig. S9). Moreover, their

morphology transformed from aggregates of small nano-crystallites (1 and 10 min) to stacked nanoplates with irregular shapes (30 and 60 min).

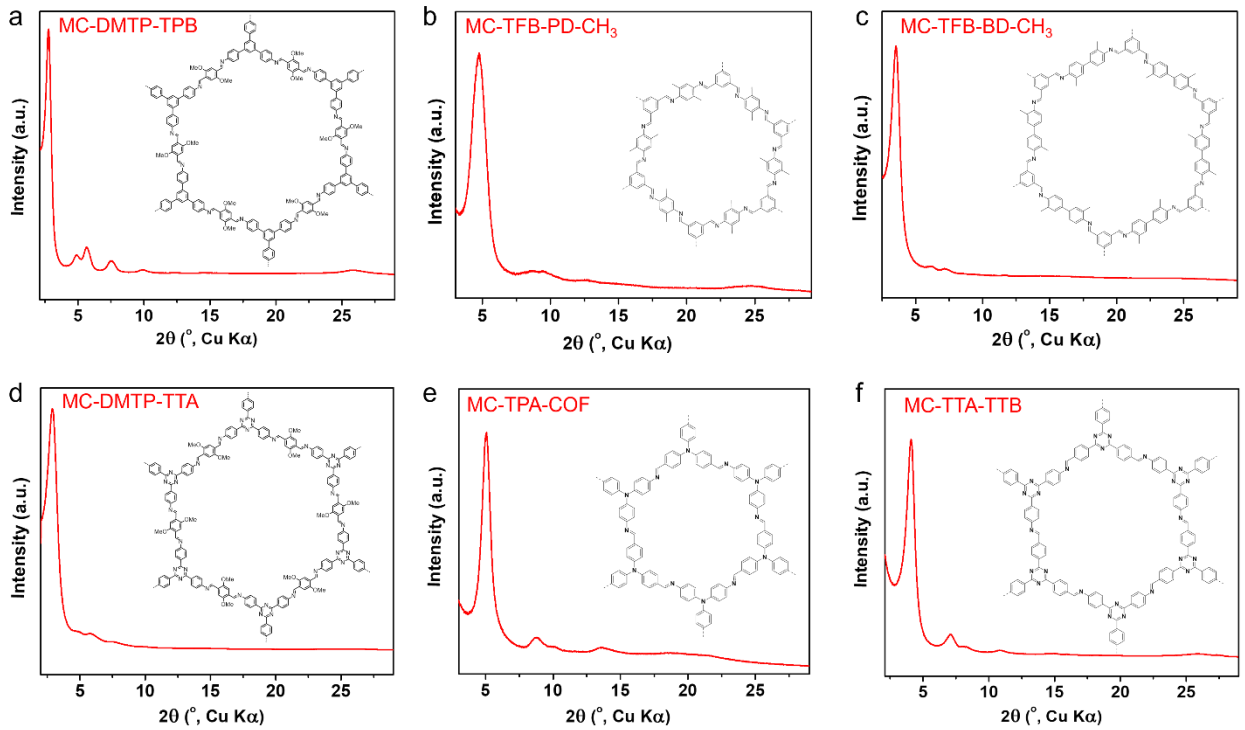

Fig. 3. PXRD patterns of imine-linked 2D COFs made through the LAG mechanochemistry. (a) MC-DMTP-TPB, (b) MC-TFB-PD-CH_3, (c) MC-TFB-BD-CH_3, (d) MC-DMTP-TTA, (e) MC-TPA-COF, and (f) MC-TTA-TTB.

To demonstrate the generality of the present mechanochemical methodology, we synthesized five additional hexagonal COFs using different combinations of C_2 + C_3 or C_3 + C_3 monomers (Scheme 1). Three of the COFs (i.e., DMTP-TTA COF,[47] TPA-COF,[48] and TTA-TTB COF[49]) have been previously reported using conventional solvothermal methods. All COFs (MC-COFs) were mechanochemically synthesized in high yields (85-98%) in just 1 hour with high crystallinities and moderate-to-high BET surface areas (Fig. 3). The optimum conditions for the mechanochemical synthesis of each COF are as follows (All synthetic procedures can be found in the supporting information): MC-TFB-PD-CH_3 COF was obtained by milling 1,3,5-triformylbenzene (TFB) and 2,5-dimethyl-1,4-phenylenediamine (PD-CH_3) using *n*-butanol as the LAG additive (η = 0.70 µL/mg, Figs. 3b and S10). MC-TFB-BD-CH_3 COF was made by milling TFB and o-tolidine using mesitylene as the LAG additive (η = 0.89 µL/mg, Figs. 3c and S11). MC-DMTP-TTA COF was composed of DMTP and 4,4′,4′′-(1,3,5-triazine-2,4,6-triyl) trianiline (TTA) using mesitylene as the LAG additive (η = 0.88 µL/mg, Figs. 3d and S12). MC-TPA COF was constructed by milling tris(4-formylphenyl) amine and tris(4-aminophenyl) amine using mesitylene as the LAG additive (η = 0.93 µL/mg, Figs. 3e and S13). MC-TTA-TTB COF was made by milling TTA and 2,4,6-tris(4-formylphenyl)-1,3,5-triazine (TTB) using acetonitrile as the LAG additive (η = 0.80 µL/mg, Figs. 3f and S14). The resultant MC-COFs were fully characterized by PXRD (Fig. 3), SEM (Figs. S15-S17), FTIR (Fig. S18), TGA (Fig. S19), and N_2 sorption analyses (Figs. S20).

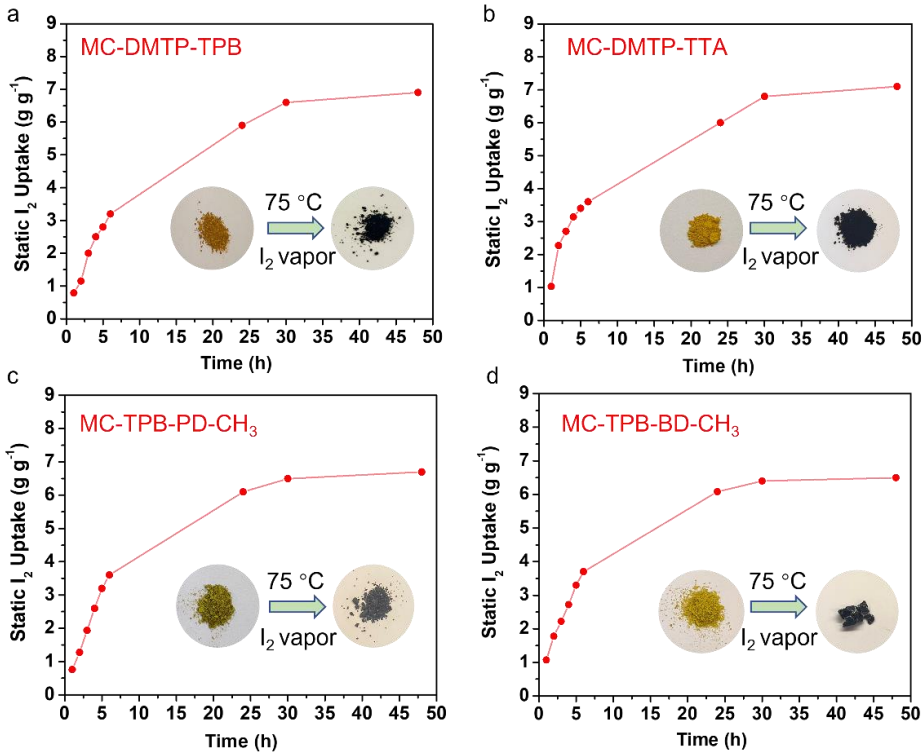

Fig. 4. The gravimetric iodine uptake of MC-COFs as a function of exposure time at 75 °C and ambient pressure. (a) MC-DMTP-TPB COF. (b) MC-DMTP-TTA COF. (c) MC-TFB-PD-CH_3 COF, and (d) MC-TFB-BD-CH_3 COF. Insets are digital photos of MC-COFs before and after iodine vapor capture.

Having six MC-COFs in hand, we sought to evaluate their performance in iodine vapor adsorption under ambient pressure at 75 °C. After the initial assessment, four MC-COFs, i.e., MC-DMTP-TPB, MC-DMTP-TTA, MC-TFB-PD-CH_3, and MC-TFB-BD-CH_3, emerged as exceptional iodine adsorbents (Fig. 4). When exposed to iodine vapor, the pristine COFs gradually changed color from yellow to black (Fig. 4, inset), indicating successful iodine adsorption by COFs. This was further confirmed by the X-ray photoelectron spectroscopy (XPS) survey spectra of COF after iodine adsorption, which exhibited two sets of intense I_{3d} peaks (Fig. S21). As depicted in Fig. 4a, MC-DMTP-TPB COF displayed rapid iodine adsorption during the first 6 hours and reached equilibrium at 6.9 g g^{-1} within 36 hours. Impressively, the iodine adsorption capacity of MC-DMTP-TPB COF surpassed the solvothermal counterpart (6.4 g g^{-1}, Fig. S22), which was synthesized using hazardous solvent under vacuum at 120 °C for 3 days. This iodine-sorbing value is also far superior to those of most reported COF adsorbents that demand long synthetic times, elevated temperatures, and toxic organic solvents (see Table S2 for detailed comparison). Moreover, the average adsorption rate, $K_{80\%}$ ($K_{80\%}$ = 80% of saturated adsorption capacity/adsorption time), was used to evaluate the adsorption kinetics.[50] MC-DMTP-TPB exhibited a higher $K_{80\%}$ value (0.26 g g h^{-1}) than the reported value (0.17 g g h^{-1}) of its solvothermal counterpart.[13] To further analyze the iodine adsorption kinetics, we adopted pseudo-first-order and pseudo-second-order kinetic models.[51] It was found that the iodine adsorption behavior in MC-DMTP-TPB COF is more suitable for the pseudo-second-order kinetic model (Figure S23), implying that chemical adsorption is the major process.[52] In addition to MC-DMTP-TPB COF, the isoreticular MC-DMTP-TTA COF with an analogous structure but more nitrogen content exhibited a slightly enhanced iodine adsorption capacity of 7.1 g g^{-1} and $K_{80\%}$ rate of 0.27 g g h^{-1} (Fig. 4b). Moreover, MC-TFB-PD-CH_3 and MC-TFB-BD-CH_3 COFs exhibited high iodine adsorption capacities of 6.4 and 6.5 g g^{-1}, respectively, accompanied by $K_{80\%}$ rates of 0.29 g g h^{-1} and 0.30 g g h^{-1} (Figs. 4c and 4d).

Recyclability is an essential factor for the practical application of COF adsorbents, as it can offset their high cost. We tested the recyclability of MC-DMTP-TPB in successive adsorption-desorption cycles. To regenerate its adsorption capacity, the adsorbed iodine in MC-DMTP-TPB COF was removed by thermal outgassing under vacuum at 135 °C overnight. MC-DMTP-TPB COF

maintained a high iodine adsorption capacity of > 5.8 g g^{-1} after three cycles, corresponding to an 87.8% recycling percentage (Fig. S24). PXRD pattern of I_2@MC-DMTP-TPB COF indicated the loss of long-range order, presumably due to the adsorbed iodine.[26, 53-54] After thermal treatment overnight, the regenerated MC-DMTP-TPB COF still showed a featureless XRD pattern (Fig. S25), which is similar to previous reports.[19, 25, 55-56] FTIR analysis verified the chemical integrity of the used MC-DMTP-TPB COF (Fig. S26). Moreover, SEM images indicated that the morphology of COF remained nearly unchanged after the recycling test (Fig. S27). These findings demonstrate that MC-DMTP-TPB COF, which was synthesized by a green mechanochemical route, proved to be a benchmark porous iodine adsorbent that combines high uptake capacity, reusability, rapid synthesis, and eco-friendliness, a combination of features that remain a grand challenge to achieve in COF adsorbents to date (Table S2).

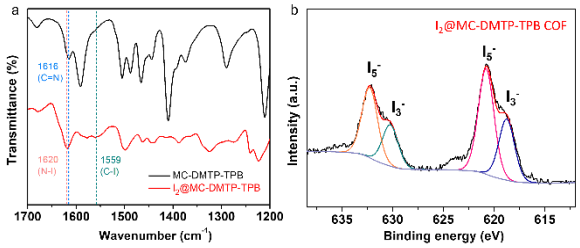

Fig. 5. (a) FTIR and (b) I3d XPS spectra of I_2@MC-DMTP-TPB COF.

To gain a better understanding of the mechanism behind the iodine adsorption in MC-COFs, we performed FTIR, XPS, and PXRD analyses of COF before and after iodine saturation. Upon iodine adsorption by MC-DMTP-TPB COF, the intensity of characteristic C=N stretch at 1615 cm^{-1} in the FTIR spectrum attenuated significantly, and two new bands emerged at 1620 and 1559 cm^{-1}, suggesting the possible formation of N-I and C-I bonds, respectively (Fig. 5a).[23] Such charge transfer between iodine and COF was further corroborated by the XPS analysis. The N 1s XPS spectrum of MC-DMTP-TPB COF displayed main binding energy at 398.4 eV arising from imine N atoms. Upon iodine adsorption, a new peak emerged at 400.5 eV (Fig. S28), which was attributed to the charge-transfer species formed between iodine and imine N atoms. As depicted in Fig. 5b, the I3d XPS spectra of I_2@MC-DMTP-TPB COF exhibited I $3d_{3/2}$ binding energies at 632.3 and 630.3 eV, as well as I $3d_{5/2}$ signals at 620.8 and 618.8 eV, corresponding to the polyiodide species (i.e., I_3^- and I_5^-) in the COF.[55] The quantitative analysis indicated that I_3^- and I_5^- species accounted for 38% and 62% of the total iodine in I_2@MC-DMTP-TPB COF. To gain further insights into the iodine adsorption behavior in COFs, we conducted XPS analysis of I_2@MC-DMTP-TPB exposed to iodine vapor at different times (Figure S29). Notably, within just 10 seconds of exposure to iodine vapor, the formation of polyiodides (i.e., I_3^- and I_5^-) was observed, with I_3^- as the dominant species (77% of the total iodine species). As the exposure time increased, the percentage of I_3^- anions gradually decreased, while I_5^- anions steadily increased. After 15 minutes of iodine exposure, the amounts of I_3^- and I_5^- anions were almost equivalent. This can be attributed to the formation of I_5^- through the reaction of I_3^- anions and neutral I_2 ($I_3^- + I_2 = I_5^-$).[57] Moreover, the PXRD pattern of I_2@MC-DMTP-TPB did not exhibit any characteristic diffraction peaks of molecular iodine (Figure S30), suggesting the transformation of iodine to polyiodides within the COF.[26]

Conclusions

In summary, we have developed a green liquid-assisted mechanochemical synthesis of imine-linked COFs, which acted as highly efficient adsorbents for static iodine vapor capture. In contrast to previous traditional solvothermal methods affording COF adsorbents, our methodology is green, rapid, efficient, generalizable, and potentially scalable, empowering the synthesis of a wide range of hexagonal COFs with varied pore sizes and functionalities within an hour. Notably, MC-DMTP-TPB COF represents a rare COF that attains high crystallinity and surface area of 1387 m^2 g^{-1} within merely 1 minute and at ambient temperature. When implemented as adsorbents for static iodine vapor capture at 75 °C, four out of the six MC-COFs exhibited exceptional iodine adsorption capacities of 6.4-7.1 g g^{-1}, surpassing those of the conventional solvothermal counterpart and most reported COF adsorbents. Furthermore, the MC-DMTP-TPB COF can be recycled three times with a high adsorption capacity (>5.8 g g^{-1}). FTIR and XPS analyses shed light on the mechanism behind the iodine adsorption by COFs. This work uncovers the immense potential of mechanochemistry towards sustainable, succinct, rapid, and scalable synthesis of COFs. These findings not only expand the toolkit for COF synthesis but also opens tremendous opportunities for a broad array of applications.

Author Contributions

N. Brown conducted the synthesis and characterization of COFs, as well as performed the iodine capture experiments. Z. Alsudairy assisted with the COF selection and the iodine capture test. R. Behera and W. Huang performed the N_2 sorption tests and data analysis. F. Akram and K. Chen assisted with SEM image acquisition. Undergraduate students K. Smith-Petty, B. Motley, and S. Williams assisted with the condition screening of COFs. C. Ingram provided support in COF characterization and offered valuable suggestions. X. Li conceived and supervised the research. N. Brown and X. Li wrote the manuscript. All authors discussed the results and edited the manuscript.

Conflicts of interest

There are no conflicts to declare.

Acknowledgements

This work was supported by the U.S. Department of Energy Early Career Award (DE-SC0022000), the National Science Foundation HBCU-UP-RIA program (2100360), and the PREM program (DMR-2122147). Part of the SEM images was acquired in the Imaging Core Facility at Georgia State University. We

thank Dr. Chongqing Yang at Shanghai Jiao Tong University for her assistance in N_2 sorption data analysis.

References

1. F. Wang, J. D. Harindintwali, Z. Yuan, M. Wang, F. Wang, S. Li, Z. Yin, L. Huang, Y. Fu and L. Li, Technologies and perspectives for achieving carbon neutrality, *The Innovation*, 2021, **2**, 100180.
2. A. Akleyev, L. Y. Krestinina, M. Degteva and E. Tolstykh, Consequences of the radiation accident at the Mayak production association in 1957 (the'Kyshtym Accident'), *J. Radiat. Prot.*, 2017, **37**, R19.
3. M. Tronko, K. Mabuchi, T. Bogdanova, M. Hatch, I. Likhtarev, A. Bouville, V. Oliynik, R. McConnell, V. Shpak and L. Zablotska, Thyroid cancer in Ukraine after the Chernobyl accident (in the framework of the Ukraine–US Thyroid Project), *J. Radiat. Prot.*, 2012, **32**, N65.
4. Y. Onda, K. Taniguchi, K. Yoshimura, H. Kato, J. Takahashi, Y. Wakiyama, F. Coppin and H. Smith, Radionuclides from the Fukushima Daiichi nuclear power plant in terrestrial systems, *Nat. Rev. Earth Environ.*, 2020, **1**, 644-660.
5. J. Huve, A. Ryzhikov, H. Nouali, V. Lalia, G. Augé and T. J. Daou, Porous sorbents for the capture of radioactive iodine compounds: a review, *RSC Adv.*, 2018, **8**, 29248-29273.
6. W. Xie, D. Cui, S.-R. Zhang, Y.-H. Xu and D.-L. Jiang, Iodine capture in porous organic polymers and metal–organic frameworks materials, *Mater. Horiz.*, 2019, **6**, 1571-1595.
7. C. S. Diercks and O. M. Yaghi, The atom, the molecule, and the covalent organic framework, *Science*, 2017, **355**, eaal1585.
8. X. Li, H. Wang, H. Chen, Q. Zheng, Q. Zhang, H. Mao, Y. Liu, S. Cai, B. Sun and C. Dun, Dynamic covalent synthesis of crystalline porous graphitic frameworks, *Chem*, 2020, **6**, 933-944.
9. X. Li, sp 2 carbon-conjugated covalent organic frameworks: synthesis, properties, and applications, *Mater. Chem. Front.*, 2021, **5**, 2931-2949.
10. Z. Alsudairy, N. Brown, A. Campbell, A. Ambus, B. Brown, K. Smith-Petty and X. Li, Covalent organic frameworks in heterogeneous catalysis: recent advances and future perspective, *Mater. Chem. Front.*, 2023, DOI: 10.1039/D3QM00188A.
11. R. Li, X. Tang, J. Wu, K. Zhang, Q. Zhang, J. Wang, J. Zheng, S. Zheng, J. Fan, W. Zhang, X. Li and S. Cai, A sulfonate-functionalized covalent organic framework for record-high adsorption and effective separation of organic dyes, *J. Chem. Eng.*, 2023, **464**, 142706.
12. Z.-J. Yin, S.-Q. Xu, T.-G. Zhan, Q.-Y. Qi, Z.-Q. Wu and X. Zhao, Ultrahigh volatile iodine uptake by hollow microspheres formed from a heteropore covalent organic framework, *Chem. Commun.*, 2017, **53**, 7266-7269.
13. P. Wang, Q. Xu, Z. Li, W. Jiang, Q. Jiang and D. Jiang, Exceptional iodine capture in 2D covalent organic frameworks, *Adv. Mater.*, 2018, **30**, 1801991.
14. M. Zhou, Z. Li, A. Munyentwali, C. Li, H. Shui and H. Li, Highly Conjugated Two‐dimensional Covalent Organic Frameworks for Efficient Iodine Uptake, *Chem. Asian J.*, 2022, **17**, e202200358.
15. Z. Alsudairy, N. Brown, C. Yang, S. Cai, F. Akram, A. Ambus, C. Ingram and X. Li, Facile Microwave-Assisted Synthesis of 2D Imine-Linked Covalent Organic Frameworks for Exceptional Iodine Capture, *Precis. Chem.*, 2023, **1**, 233-240.
16. Y. Zhang, W. Shi, Y. Zhao, C. Zhang and Y. Zhi, Linkage Design in Two-Dimensional Covalent Organic Frameworks for High Iodine Uptake, *Macromol. Rapid Commun.*, 2023, **44**, 2200787.
17. L. Zhai, S. Sun, P. Chen, Y. Zhang, Q. Sun, Q. Xu, Y. Wu, R. Nie, Z. Li and L. Mi, Constructing cationic covalent organic frameworks by a post-function process for an exceptional iodine capture via electrostatic interactions, *Mater. Chem. Front.*, 2021, **5**, 5463-5470.
18. S.-Y. Zhang, X.-H. Tang, Y.-L. Yan, S.-Q. Li, S. Zheng, J. Fan, X. Li, W.-G. Zhang and S. Cai, Facile and Site-Selective Synthesis of an Amine-Functionalized Covalent Organic Framework, *ACS Macro Lett.*, 2021, **10**, 1590-1596.
19. Y.-X. Yang, X.-H. Tang, J.-L. Wu, Z.-Y. Dong, Y.-L. Yan, S.-R. Zheng, J. Fan, X. Li, S. Cai and W.-G. Zhang, Transformation of a hydrazone-linked covalent organic framework into a highly stable hydrazide-linked one, *ACS Appl. Polym. Mater.*, 2022, **4**, 4624-4631.
20. X. Yan, Y. Yang, G. Li, J. Zhang, Y. He, R. Wang, Z. Lin and Z. Cai, Thiophene-based covalent organic frameworks for highly efficient iodine capture, *Chin. Chem. Lett.*, 2023, **34**, 107201.
21. J. Chang, H. Li, J. Zhao, X. Guan, C. Li, G. Yu, V. Valtchev, Y. Yan, S. Qiu and Q. Fang, Tetrathiafulvalene-based covalent organic frameworks for ultrahigh iodine capture, *Chem. Sci.*, 2021, **12**, 8452-8457.
22. Y. Li, X. Li, J. Li, G. Cheng and H. Ke, Phosphine-based covalent organic framework for highly efficient iodine capture, *Microporous Mesoporous Mater.*, 2021, **325**, 111351.
23. Y. Xie, T. Pan, Q. Lei, C. Chen, X. Dong, Y. Yuan, J. Shen, Y. Cai, C. Zhou and I. Pinnau, Ionic Functionalization of Multivariate Covalent Organic Frameworks to Achieve an Exceptionally High Iodine‐Capture Capacity, *Angew. Chem. Int. Ed.*, 2021, **60**, 22432-22440.
24. D. Zhu, Y. Zhu, Q. Yan, M. Barnes, F. Liu, P. Yu, C.-P. Tseng, N. Tjahjono, P.-C. Huang, M. M. Rahman, E. Egap, P. M. Ajayan and R. Verduzco, Pure Crystalline Covalent Organic Framework Aerogels, *Chem. Mater.*, 2021, **33**, 4216-4224.
25. X. Li, Z. Jia, J. Zhang, Y. Zou, B. Jiang, Y. Zhang, K. Shu, N. Liu, Y. Li and L. Ma, Moderate and Universal Synthesis of Undoped Covalent Organic Framework Aerogels for Enhanced Iodine Uptake, *Chem. Mater.*, 2022, **34**, 11062-11071.
26. T. Liu, Y. Zhao, M. Song, X. Pang, X. Shi, J. Jia, L. Chi and G. Lu, Ordered Macro–Microporous Single Crystals of Covalent Organic Frameworks with Efficient Sorption of Iodine, *J. Am. Chem. Soc.*, 2023, **145**, 2544-2552.
27. X. Li, C. Yang, B. Sun, S. Cai, Z. Chen, Y. Lv, J. Zhang and Y. Liu, Expeditious synthesis of covalent organic frameworks: a review, *J. Mater. Chem. A.*, 2020, **8**, 16045-16060.
28. J. Á. Martín-Illán, D. Rodríguez-San-Miguel, C. Franco, I. Imaz, D. Maspoch, J. Puigmartí-Luis and F. Zamora, Green synthesis of imine-based covalent organic frameworks in water, *Chem. Commun.*, 2020, **56**, 6704-6707.
29. Y. Chen, W. Li, X.-H. Wang, R.-Z. Gao, A.-N. Tang and D.-M. Kong, Green synthesis of covalent organic frameworks based on reaction media, *Mater. Chem. Front.*, 2021, **5**, 1253-1267.
30. J.-L. Do and T. Friščić, Mechanochemistry: a force of synthesis, *ACS Cent. Sci.*, 2017, **3**, 13-19.
31. F. Gomollón-Bel, Ten Chemical Innovations That Will Change Our World: IUPAC identifies emerging technologies in Chemistry with potential to make our planet more sustainable, *Chem. Int.*, 2019, **41**, 12-17.
32. S. L. James, C. J. Adams, C. Bolm, D. Braga, P. Collier, T. Friščić, F. Grepioni, K. D. Harris, G. Hyett and W. Jones,

Mechanochemistry: opportunities for new and cleaner synthesis, *Chem. Soc. Rev.*, 2012, **41**, 413-447.
33. B. Szczęśniak, S. Borysiuk, J. Choma and M. Jaroniec, Mechanochemical synthesis of highly porous materials, *Mater. Horiz.*, 2020, **7**, 1457-1473.
34. P. Zhang and S. Dai, Mechanochemical synthesis of porous organic materials, *J. Mater. Chem. A.*, 2017, **5**, 16118-16127.
35. T. Stolar and K. Užarević, Mechanochemistry: an efficient and versatile toolbox for synthesis, transformation, and functionalization of porous metal–organic frameworks, *CrystEngComm*, 2020, **22**, 4511-4525.
36. B. P. Biswal, S. Chandra, S. Kandambeth, B. Lukose, T. Heine and R. Banerjee, Mechanochemical synthesis of chemically stable isoreticular covalent organic frameworks, *J. Am. Chem. Soc.*, 2013, **135**, 5328-5331.
37. G. Das, D. B. Shinde, S. Kandambeth, B. P. Biswal and R. Banerjee, Mechanosynthesis of imine, β-ketoenamine, and hydrogen-bonded imine-linked covalent organic frameworks using liquid-assisted grinding, *Chem. Commun.*, 2014, **50**, 12615-12618.
38. S. Karak, S. Kandambeth, B. P. Biswal, H. S. Sasmal, S. Kumar, P. Pachfule and R. Banerjee, Constructing Ultraporous Covalent Organic Frameworks in Seconds via an Organic Terracotta Process, *J. Am. Chem. Soc.*, 2017, **139**, 1856-1862.
39. S. T. Emmerling, L. S. Germann, P. A. Julien, I. Moudrakovski, M. Etter, T. Friščić, R. E. Dinnebier and B. V. Lotsch, In situ monitoring of mechanochemical covalent organic framework formation reveals templating effect of liquid additive, *Chem*, 2021, **7**, 1639-1652.
40. D. B. Shinde, H. B. Aiyappa, M. Bhadra, B. P. Biswal, P. Wadge, S. Kandambeth, B. Garai, T. Kundu, S. Kurungot and R. Banerjee, A mechanochemically synthesized covalent organic framework as a proton-conducting solid electrolyte, *J. Mater. Chem. A.*, 2016, **4**, 2682-2690.
41. A. Khayum M, V. Vijayakumar, S. Karak, S. Kandambeth, M. Bhadra, K. Suresh, N. Acharambath, S. Kurungot and R. Banerjee, Convergent Covalent Organic Framework Thin Sheets as Flexible Supercapacitor Electrodes, *ACS Appl. Mater. Interfaces*, 2018, **10**, 28139-28146.
42. X. Wang, R. Ma, L. Hao, Q. Wu, C. Wang and Z. Wang, Mechanochemical synthesis of covalent organic framework for the efficient extraction of benzoylurea insecticides, *J. Chromatogr. A*, 2018, **1551**, 1-9.
43. R. Gao, N. Zhong, L. Tong, X. Kou, W. Huang, H. Yang, S. Huang, J. Wu, G. Chen and G. Ouyang, Mechanochemistry-guided reticular assembly for stabilizing enzymes with covalent organic frameworks, *Cell Rep. Phys. Sci.*, 2022, **3**, 101153.
44. H. Xu, J. Gao and D. Jiang, Stable, crystalline, porous, covalent organic frameworks as a platform for chiral organocatalysts, *Nat. Chem.*, 2015, **7**, 905-912.
45. Y. Chen, H. Wu, Z. Liu, X. Sun, Q. Xia and Z. Li, Liquid-assisted mechanochemical synthesis of copper based MOF-505 for the separation of CO2 over CH4 or N2, *Ind. Eng. Chem. Res.*, 2018, **57**, 703-709.
46. X. Li, C. Zhang, S. Cai, X. Lei, V. Altoe, F. Hong, J. J. Urban, J. Ciston, E. M. Chan and Y. Liu, Facile transformation of imine covalent organic frameworks into ultrastable crystalline porous aromatic frameworks, *Nat. Commun.*, 2018, **9**, 2998.
47. Y. Zhi, Z. Li, X. Feng, H. Xia, Y. Zhang, Z. Shi, Y. Mu and X. Liu, Covalent organic frameworks as metal-free heterogeneous photocatalysts for organic transformations, *J. Mater. Chem. A.*, 2017, **5**, 22933-22938.
48. Y. Peng, Y. Huang, Y. Zhu, B. Chen, L. Wang, Z. Lai, Z. Zhang, M. Zhao, C. Tan and N. Yang, Ultrathin two-dimensional covalent organic framework nanosheets: preparation and application in highly sensitive and selective DNA detection, *J. Am. Chem. Soc.*, 2017, **139**, 8698-8704.
49. V. S. Vyas, M. Vishwakarma, I. Moudrakovski, F. Haase, G. Savasci, C. Ochsenfeld, J. P. Spatz and B. V. Lotsch, Exploiting noncovalent interactions in an imine ‐ based covalent organic framework for quercetin delivery, *Adv. Mater.*, 2016, **28**, 8749-8754.
50. J. Fu, J.-Y. Liu, G.-H. Zhang, Q.-H. Zhu, S.-L. Wang, S. Qin, L. He and G.-H. Tao, Boost of Gas Adsorption Kinetics of Covalent Organic Frameworks via Ionic Liquid Solution Process, *Small*, **n/a**, 2302570.
51. Y.-Q. Xiang, Y.-H. Wang, H. Chen, J. Fu, Q.-H. Zhu, X.-L. Yang, X.-H. Xu, S. Qin, L. He and G.-H. Tao, Efficient enrichment of iodine by supported ionic liquid with three effective adsorption sites: Heteroatoms, fused aromatic rings and ionic bond, *J. Chem. Eng.*, 2023, **456**, 140979.
52. X. Guo, Y. Tian, M. Zhang, Y. Li, R. Wen, X. Li, X. Li, Y. Xue, L. Ma, C. Xia and S. Li, Mechanistic Insight into Hydrogen-Bond-Controlled Crystallinity and Adsorption Property of Covalent Organic Frameworks from Flexible Building Blocks, *Chem. Mater.*, 2018, **30**, 2299-2308.
53. L. He, L. Chen, X. Dong, S. Zhang, M. Zhang, X. Dai, X. Liu, P. Lin, K. Li and C. Chen, A nitrogen-rich covalent organic framework for simultaneous dynamic capture of iodine and methyl iodide, *Chem*, 2021, **7**, 699-714.
54. Y. Xie, T. Pan, Q. Lei, C. Chen, X. Dong, Y. Yuan, W. A. Maksoud, L. Zhao, L. Cavallo, I. Pinnau and Y. Han, Efficient and simultaneous capture of iodine and methyl iodide achieved by a covalent organic framework, *Nat. Commun.*, 2022, **13**, 2878.
55. C. Liu, Y. Jin, Z. Yu, L. Gong, H. Wang, B. Yu, W. Zhang and J. Jiang, Transformation of Porous Organic Cages and Covalent Organic Frameworks with Efficient Iodine Vapor Capture Performance, *J. Am. Chem. Soc.*, 2022, **144**, 12390-12399.
56. C. Wang, Y. Wang, R. Ge, X. Song, X. Xing, Q. Jiang, H. Lu, C. Hao, X. Guo, Y. Gao and D. Jiang, A 3D Covalent Organic Framework with Exceptionally High Iodine Capture Capability, *Chem. Eur. J.*, 2018, **24**, 585-589.
57. W. Salaneck, H. Thomas, R. Bigelow, C. Duke, E. Plummer, A. Heeger and A. MacDiarmid, Photoelectron spectroscopy of iodine ‐ doped polyacetylene, *J. Chem. Phys.*, 1980, **72**, 3674-3678.